Instability of a Lamellar Phase under Shear Flow: Formation of Multilamellar Vesicles

L. Courbin, J. P. Delville, J. Rouch, and P. Panizza*

Centre de Physique Moléculaire Optique et Hertzienne, UMR CNRS 5798, Université Bordeaux I,
351 Cours de la Libération, 33400 Talence, France

The formation of closed-compact multilamellar vesicles (referred to in the literature as the "onion texture") obtained upon shearing lamellar phases is studied using small-angle light scattering and cross-polarized microscopy. By varying the shear rate $\dot{\gamma}$, the gap cell D, and the smectic distance d, we show that: (i) the formation of this structure occurs homogeneously in the cell at a well-defined wave vector q_i, via a strain-controlled process, and (ii) the value of q_i varies as $(d\dot{\gamma}/D)^{1/3}$. These results strongly suggest that formation of multilamellar vesicles may be monitored by an undulation (buckling) instability of the membranes, as expected from theory.

Lyotropic lamellar phases consist of a periodical stacking of flexible fluid membranes intercalated by solvent [1]. Since the lamellae are very flexible, the structure of these phases can be strongly affected by weak shear flows [2]. Above a critical shear rate, they undergo a transformation leading to a state of monodisperse multilayered vesicles (MLVs) referred to in the literature as "onion texture" [3]. A wide amount of work has been performed to describe and characterize the couplings between structure and flow in such systems [4–8]. Yet the physical mechanism of the formation of MLVs is still under debate. A few years ago, inspired by the pioneering work of Oswald *et al.* on smectic-*A* phases [9], some authors have conjectured that it may result from the existence of a nonuniform gap spacing [2,10,11]. In equilibrium, this spatial variation in the gap is accommodated by the existence of dislocations which can move at low shear rates. However, when the shear rate becomes too high, these dislocations cannot follow the flow any more and this gives rise to a dilative strain perpendicular to the layers, triggering the buckling (or undulation) instability. Because of its resistance to the flow, the buckling pattern cannot sustain flow and likely rolls up into MLVs. Recently, Zilman and Granek [12] have proposed another buckling mechanism which exists even at a uniform gap, based on the coupling between thermal undulations of the membranes and the flow. According to them, the suppression by the flow of the short wavelength membrane undulations [13,14] responsible of the membrane excess area generates an effective lateral pressure. Above a critical shear rate, this pressure can no longer be balanced by the elastic forces of the lamellae and leads to a buckling instability similar to that obtained by dilative strain.

So far, very few experiments have focused on the dynamics of formation of MLVs. Bergenholtz and Wagner [4] and Zipfel *et al.* [15] have shown that the formation of onions is strain-controlled but they have not identified the exact nature of this mechanism. On the other hand, Léon *et al.* [7] conclude that the shear-induced gelation they

observed in a dilute lamellar system made of sodium bis(2-ethylhexyl) sulfosuccinate (AOT) and brine occurs via a nucleation process, a result which is in contradiction with theoretical expectations [3,10–12,16]. As is evident, the nature of the mechanism leading to MLVs remains still unclear and deserves further investigation. To elucidate this, we study the formation of MLVs in a lamellar phase stabilized by undulation interaction, using rheophysics techniques, small-angle light scattering (SALS), and optical microscopy.

Experiments.—The experiments are performed in a quaternary liquid mixture made of sodium dodecylsulfate (SDS), pentanol, dodecane, and water. For a water/SDS ratio of 1.55, the phase diagram of the mixture [17] exhibits a very large lamellar domain. We prepare an initial lamellar phase whose composition in weight fraction is 15.1% SDS, 23.35% water, 14.55% pentanol, and 47% dodecane. This phase is stabilized by undulation interactions [18] and its smectic distance, d, can be continuously changed by dilution with the solvent (91% wt dodecane and 9% wt pentanol) from typically 50 up to a few hundreds of Å. Using small-angle x-ray scattering [19], it has been shown that the logarithmic correction due to the excess area induced by the strong thermal fluctuation of the flexible membranes leads to the following variation of d, with the membrane volume fraction, ϕ_m:

$$d(\text{Å}) = \frac{35.6 - 7.9\ln(\phi_m)}{\phi_m}. \tag{1}$$

Along this dilution line, the membrane thickness δ remains fixed ($\delta = 26$ Å) and the membrane bending modulus is about $\kappa \approx 0.2 k_B T$ [19], where $k_B T$ is the thermal energy. The effect of shear flow in this system is summarized in a so-called shear diagram [3]. At low shear rates, the lamellae are mainly oriented perpendicular to the shear gradient direction. Above a critical shear rate $\dot{\gamma}_c$, they roll up to form closed-compact MLVs (onion

texture). Their size is fixed by $\dot{\gamma}$ and can vary from a few μm to a tenth of it.

SALS experiments are performed under shear flow with a homemade transparent Couette cell [8]. The fixed inner cylinder of radius 25 mm is cone shaped at its lower end. The outer cylinder rotates at constant angular velocity ω and can be changed in order to obtain narrow gaps D, ranging from 0.5 to 2 mm. Both cylinders are thermostated at $T = 25.0 \pm 0.1\,°C$ using a water bath. A circularly polarized He-Ne laser beam (wavelength $\lambda = 632.8$ nm in vacuum) passes through the cell along the shear gradient direction and probes the sample in only one of the gaps. The unpolarized scattered pattern corresponding to light scattered in the velocity-vorticity $(\vec{V}, \vec{Z})$ plane is digitized, by means of a CCD video camera coupled to a computer for the frame acquisition. Two linear electrodes mounted diametrically on the stator and connected to a Hewlett Packard 4192 impedance analyzer allow us to follow the variation with time and shear rate of the electrical conductivity along the velocity direction [20].

The lamellar phase is stirred and then left at rest for about a week to ensure equilibrium. Then the solution is poured into the Couette cell and sheared at a constant shear rate (typically $\dot{\gamma}_p = 0.4$ s^{-1}) below the threshold $\dot{\gamma}_c$ (of the order of 1 s^{-1}) above which MLVs form, until the corresponding steady state (oriented lamellae) is reached. Conductivity measurements and SALS experiments performed under flow enable us to check that this initial oriented steady state is obtained; i.e., the conductivity becomes constant and no ring, characteristic of the onion texture, is observed in the SALS pattern. Then in order to form MLVs, the shear rate is suddenly increased to a value $\dot{\gamma} \geq \dot{\gamma}_c$. This procedure allows us to follow the MLVs' formation from an oriented lamellar state with reproducible initial conditions.

Results.—Figure 1 shows the evolution of the SALS pattern following such a quench in shear rate for $d = 95$ Å and $D = 1$ mm. First, in agreement with observations made by Zipfel *et al.* on another lamellar system [15], we observe a strong enhancement of the intensity scattered at very small angles, the scattering pattern being slightly elongated along the vorticity direction. After a well-defined time delay t_e, a Bragg ring appears suddenly at a finite wave vector $q = q_i$, indicating the emergence of a characteristic length scale in the solution. Note that, once the shear rate is stopped, this ring persists with the same radius for at least a few hours. Optical microscopy has been performed under shear (*in situ*) using a commercial rheovisiometer with a cone-plate cell [20]. Observations, made at t_e between crossed polarizers, reveal a homogeneous modulation of the optical index in the whole cell [Fig. 2(b)] exhibiting a characteristic wavelength $R_i = 2\pi/q_i$. This texture [Fig. 2(b)] is characteristic of an assembly made of monodisperse closed-compact MLVs of size R_i [3]. Upon a further shearing, the
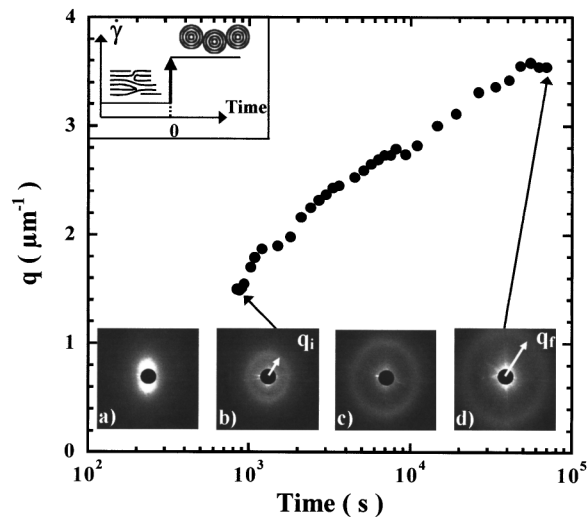

FIG. 1. Emergence and growth of the Bragg peak, q, as a function of time when $\dot{\gamma} = 6$ s^{-1} is applied to a L_α phase with $d = 95$ Å which has been previously sheared at 0.4 s^{-1} for 12 h. $t = 0$ corresponds to the quench in shear rate (see inset). Insets: SALS patterns observed in the $(\vec{V}, \vec{Z})$ plane (a) $t = 450$ s, (b) $t = t_e = 880$ s, (c) $t = 9300$ s, and (d) $t = 69\,000$ s. t_e corresponds to the time at which the scattering ring first appears; q_i is its position.

scattering ring moves continuously to larger wave vectors until it reaches its final position, q_f. This shift shows that once the closed-compact vesicles are formed, their size decreases continuously until a mechanical balance between viscous and elastic stresses is reached [Figs. 2(c) and 2(d)]. On the other hand, observations made under shear flow just before t_e do not reveal the presence of large
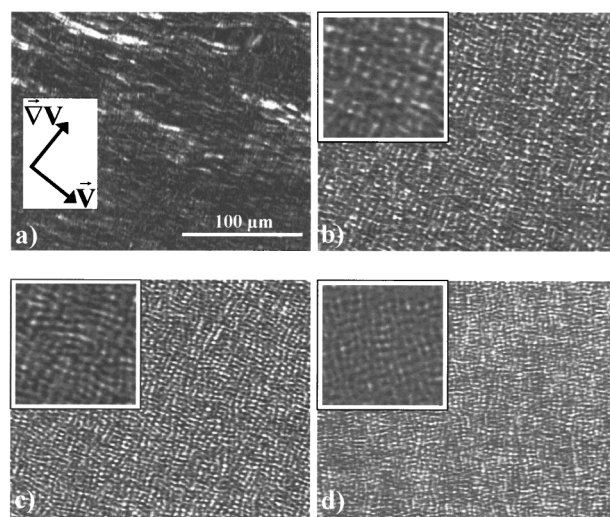

FIG. 2. Optical microscopy images of the L_α phase obtained in the rheovisiometer at different times t after $\dot{\gamma} = 8$ s^{-1} is applied: (a) for $t < t_e$, (b) at $t = t_e$, (c) for $t > t_e$, and before reaching the final steady state (d) after reaching the final size. Magnification is ($\times 10$) and ($\times 20$) in insets.
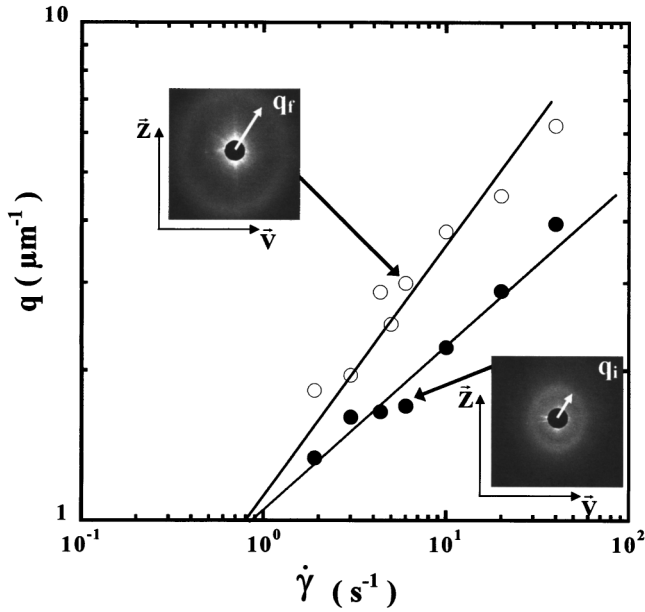
FIG. 3. Positions of the emergent and final Bragg rings, q_i (●) and q_f (○), as a function of $\dot{\gamma}$. The solid lines correspond to the best power law fits: $q_i \propto \dot{\gamma}^{1/3}$ and $q_f \propto \dot{\gamma}^{1/2}$. The system is that of Fig. 1.

isolated vesicles [Fig. 2(a)]. Contrary to Ref. [7], the formation of the onion structure in our system does not therefore occur through the nucleation of large isolated vesicles [21]. Figure 3 shows the variations of q_f and q_i versus $\dot{\gamma}$. q_f is consistent with $\dot{\gamma}^{1/2}$ as previously published [3,4], whereas q_i scales as $\dot{\gamma}^{1/3}$. In order to investigate the variation of q_i with parameters that char-
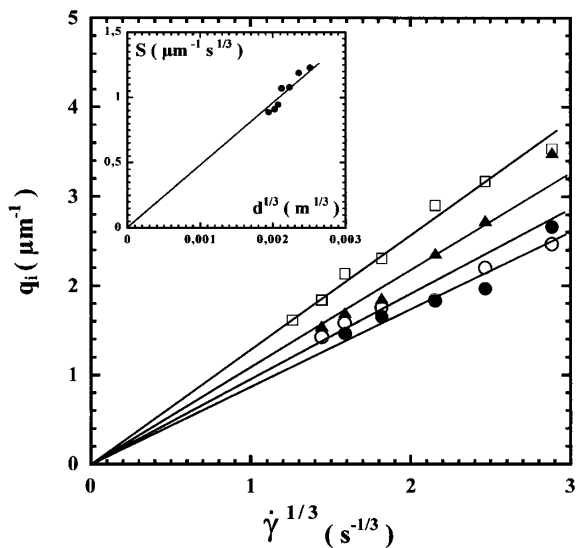

FIG. 4. Shown is q_i as a function of $\dot{\gamma}^{1/3}$ for $D = 1$ mm and for different d: (●) $d = 73$ Å, (○) $d = 89$ Å, (▲) $d = 111$ Å, and (□) $d = 159$ Å. Inset: Shown is the slope $S(d)$, which corresponds to the slope of the best linear fit: $q_i = S(d)\dot{\gamma}^{1/3}$ versus $d^{1/3}$.

acterize the system and the experimental setup, we work first with lamellar phases having different smectic distance d. For a given value of $\dot{\gamma}$, Fig. 4 shows that the value of q_i increases with d. When we plot q_i versus d, we find a $d^{1/3}$ dependence, as can be seen in the inset in Fig. 4. We then change the gap spacing D of the cell, fixing $d = 111$ Å. For a fixed shear rate, we observe that the value of q_i decreases with D and is consistent with $q_i \propto D^{-1/3}$ (see inset in Fig. 5). Finally, all results can be summarized if we plot q_i versus $(\dot{\gamma}d/D)$ (Fig. 5). In this double-logarithmic plot, all the data collapse on a master line having a slope of $1/3$: i.e., $q_i = A(\dot{\gamma}d/D)^{1/3}$. The dimension of the prefactor A corresponds to the ratio of a time by a length to the power one-third. Since it likely depends on a shear viscosity η and on an energy (likely the membrane bending modulus κ), this dimensional analysis yields to $q_i = a(\eta\dot{\gamma}d/D\kappa)^{1/3}$, where a is a numerical constant.

Discussion.—As already evidenced by Zipfel *et al.* [15], our observations demonstrate that the transition from oriented lamellar state to a state of MLVs involves at least two steps. First, an intermediate state characterized by a vertical streak in SALS is formed. This observation is compatible with the existence of an initial stripe buckling that subsequently breaks the layers and stabilizes elongated structures along the flow direction [16]. Then this intermediate state transforms into MLVs as the shear
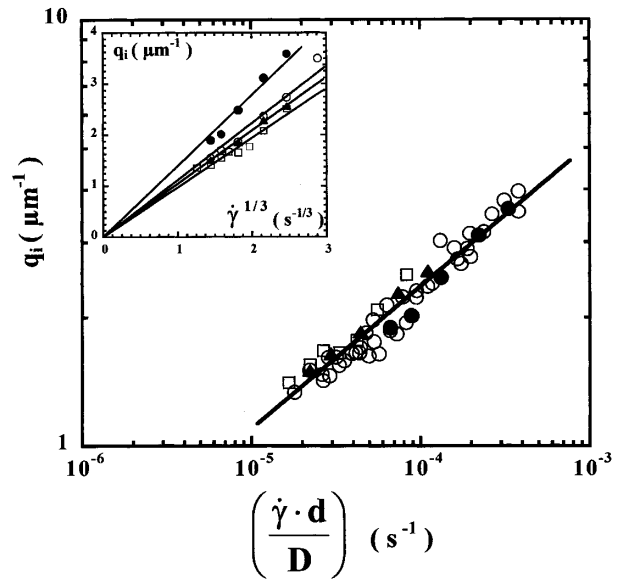

FIG. 5. Master curve: q_i represented in a log-log plot as a function of $(d\dot{\gamma}/D)$ for different d and D values: (○) $D = 1$ mm and the different values of d are 73, 83, 89, 95, 111, 131, and 159 Å, (●) $D = 0.5$ mm and $d = 111$ Å, (▲) $D = 1.5$ mm and $d = 111$ Å, and (□) $D = 2$ mm and $d = 111$ Å. The slope is consistent with $1/3$. The best fit of such a power law gives $q_i = 50(\dot{\gamma}d/D)^{1/3}$. Inset: Shown is q_i as a function of $\dot{\gamma}^{1/3}$ for $d = 111$ Å and different values of D. Symbols are identical to before.
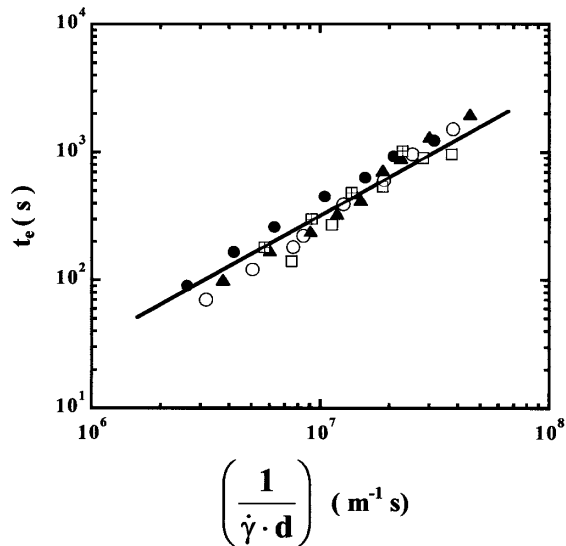
FIG. 6. Shown is t_e as a function of $(\dot{\gamma}d)^{-1}$ for different d and D: ($\bullet$) $D = 1$ mm and $d = 159$ Å, ($\circ$) $D = 1$ mm and $d = 131$ Å, ($\blacktriangle$) $D = 2$ mm and $d = 111$ Å, ($\square$) $D = 1$ mm and $d = 89$ Å, and ($\boxplus$) $D = 1$ mm and $d = 73$ Å.

continues. In agreement with several previous studies [4,15], our data indicate that this second step is strain controlled. Contrary to the results of Léon et al. [7], the MLV formation in our system is not due to a nucleation of large isolated vesicles but occurs homogeneously in the cell at a given wave vector, q_i. A systematic study of t_e, the time necessary to reach the critical strain $\gamma_e = \dot{\gamma}t_e$ required to form MLVs, shows that γ_e does not depend on the gap spacing D and varies as the inverse of d (Fig. 6). The expression of q_i, obtained from dimensional arguments, bears striking similarities to that derived by Zilman and Granek [12] for the most unstable wave vector of the so-called buckling effect. Using a nonlinear analysis, these authors have shown that above the instability threshold (i.e., for $\dot{\gamma} \geq \dot{\gamma}_c$), the buckling wavelength varies as

$$q_B = b\dot{\gamma}^{1/3}\left[\frac{\eta^2\tilde{B}d^4}{KD^2(k_BT)^2}\right]^{1/6}, \qquad (2)$$

where $\tilde{B}$, K, and b represent, respectively, the compression modulus at constant chemical potential, the smectic splay constant, and a numerical factor which depends on the lattice used in their model. Our dimensional analysis leads to a result in fairly good agreement with Eq. (2), if one recalls that for a lamellar phase stabilized by undulations [22]:

$$\tilde{B} = \frac{9\pi^2(k_BT)^2}{64\kappa}d^{-3} \quad \text{and} \quad K = \kappa/d. \qquad (3)$$

For our system, all the parameters involved in Eqs. (2) and (3) are known. Using $\kappa \approx 0.2k_BT$, $\eta \approx 10^{-2}$ Pa $\cdot$ s,

and taking $b = 2.6$ (for a stripe buckling [22]), we get from Eq. (2) $q_B \approx 7(\dot{\gamma}d/D)^{1/3}$, whereas experimental observations give $q_i \approx 50(\dot{\gamma}d/D)^{1/3}$ (see Fig. 5). To conclude, our data validate the two-step mechanism at the origin of formation of MLVs, expected from theory [3,11,12], namely, a buckling instability followed by the rolling up of the unstable buckled structure into MLVs. The formation of MLVs occurs in our system homogeneously in the shear cell at a well-defined wave vector q_i scaling like the most unstable wave vector of the primary buckling instability [11]. These striking similarities strongly suggest that the most unstable wave vector of the buckling instability monitors the initial size of MLVs, as already inferred by Zilman and Granek [12]. These very general results could have important significance for controlling and predicting the kinetics of the onion phase formation.

*Email address: ppanizza@cribx1.u-bordeaux.fr

[1] J. Israelchvili, in Physics of Amphiphiles, edited by V. Degiorgio and M. Corti (North-Holland, Amsterdam, 1985).
[2] R. Bruisma and Y. Rabin, Phys. Rev. A **45**, 994 (1992).
[3] O. Diat et al., J. Phys. II (France) **3**, 1427 (1993).
[4] J. Bergenholtz and N. J. Wagner, Langmuir **12**, 3122 (1996).
[5] J. Arrault et al., Europhys. Lett. **38**, 625 (1997).
[6] J. Berghausen et al., Europhys. Lett. **43**, 683 (1998).
[7] A. Léon et al., Phys. Rev. Lett. **84**, 1335 (2000).
[8] L. Courbin et al., Europhys. Lett. **55**, 880 (2001).
[9] P. Oswald and S. I. Ben-Abraham, J. Phys. (Paris) **43**, 1193 (1982).
[10] R. G. Larson, in The Structure and Rheology of Complex Fluids (Oxford University, New York, 1999).
[11] A. S. Wunenburger et al., Eur. Phys. J. E **2**, 277 (2000).
[12] A. G. Zilman and R. Granek, Eur. Phys. J. B **11**, 593 (1999).
[13] S. Ramaswamy, Phys. Rev. A **29**, 1506 (1984).
[14] J. Yamamoto and H. Tanaka, Phys. Rev. Lett. **74**, 932 (1995).
[15] J. Zipfel et al., Europhys. Lett. **53**, 335 (2001).
[16] S. Marlow and P. D. Olmsted, Eur. J. Phys. E (to be published).
[17] D. Roux and A. M. Bellocq, Phys. Rev. Lett. **52**, 1895 (1984).
[18] W. Helfrich, Z. Naturforsch. **33A**, 305 (1978).
[19] E. Freyssingeas, D. Roux, and F. Nallet, J. Phys. Condens. Matter **8**, 2801 (1996).
[20] P. Panizza et al., Phys. Rev. E **64**, 021502 (2001).
[21] P. M. Chaikin and T. C. Lubensky, in Principles of Condensed Matter Physics (Cambridge University, Cambridge, England, 1997).
[22] F. Nallet, D. Roux, and S. T. Milner, J. Phys. (Paris) **51**, 2333 (1990).